Journal of Power Sources 267 (2014) 255–259

Contents lists available at ScienceDirect

Journal of Power Sources

journal homepage: www.elsevier.com/locate/jpowsour

Short communication

Thermal aging of electrolytes used in lithium-ion batteries – An investigation of the impact of protic impurities and different housing materials

Patricia Handel [a, b, *], Gisela Fauler [a], Katja Kapper [a], Martin Schmuck [a], Christoph Stangl [a], Roland Fischer [b], Frank Uhlig [b], Stefan Koller [a]

[a] VARTA Micro Innovation GmbH, Stremayrgasse 9, 8010 Graz, Austria
[b] Institute of Inorganic Chemistry, Graz University of Technology, Stremayrgasse 9/V, 8010 Graz, Austria

HIGHLIGHTS

- Thermal aging of 1 M $LiPF_6$ in EC:DEC (1:2, v/v) at 60 °C and ambient temperature in two different packaging materials.
- Hardly any decomposition products are detected if aging occurred in pouch bags sealed under argon atmosphere.
- The influence of water and water-containing LFP on electrolyte aging is shown.
- Quantification of decomposition product $O{=}PF_2(OH)$ by ^{19}F NMR spectroscopy.

ARTICLE INFO

Article history:
Received 1 April 2014
Received in revised form
28 April 2014
Accepted 14 May 2014
Available online 23 May 2014

Keywords:
Lithium-ion battery
Thermal aging
Electrolyte
Lithium hexafluorophosphate

ABSTRACT

Thermal degradation products in lithium-ion batteries result mainly from hydrolysis sensitivity of lithium hexafluorophosphate ($LiPF_6$). As organic carbonate solvents contain traces of protic impurities, the thermal decomposition of electrolytes is enhanced. Therefore, resulting degradation products are studied with nuclear magnetic resonance spectroscopy (NMR) and gas chromatography mass spectrometry (GC–MS). The electrolyte contains 1 M $LiPF_6$ in a binary mixture of ethylene carbonate (EC) and diethylene carbonate (DEC) in a ratio of 1:2 (v/v) and is aged at ambient and elevated temperature. The impact of protic impurities, either added as deionized water or incorporated in positive electrode material, upon aging is investigated. Further, the influence of different housing materials on the electrolyte degradation is shown. Difluorophosphoric acid is identified as main decomposition product by NMR-spectroscopy. Traces of other decomposition products are determined by headspace GC–MS. Acid–base and coulometric titration are used to determine the total amount of acid and water content upon aging, respectively. The aim of this investigation is to achieve profound understanding about the thermal decomposition of one most common used electrolyte in a battery-like housing material.

© 2014 Elsevier B.V. All rights reserved.

1. Introduction

Since the introduction of the lithium-ion battery technology by Sony Energytech in 1990 [1], the interest among this technology has emerged steadily, not only for portable devices but also for automotive industry. Their high energy density as well as outstanding cycle stability are the main reasons for commercial success, but several problems arise with the usage of the most common electrolytes, which contain lithium hexafluorophosphate ($LiPF_6$) as conductive salt and a mixture of cyclic and non-cyclic, organic carbonates such as ethylene carbonate (EC) and diethyl carbonate (DEC) as solvent, respectively. Considering the lifetime of lithium-ion batteries, particular attention should still be paid to the electrode/electrolyte interface and the electrochemical and thermal degradation of the electrolyte. The latter contributes significantly to the long-term performance of lithium-ion batteries [2–5].

In fact, electrolyte decomposition is inevitable due to the low electrochemical potential of the charged negative electrode. However, this degradation leads to the formation of a protective, electronically isolating film on the surface of the anode, the so-called solid electrolyte interphase (SEI), which is crucial in terms of a

* Corresponding author. VARTA Micro Innovation GmbH, Stremayrgasse 9, 8010 Graz, Austria. Tel.: +43 (0)316 873 32344; fax: +43 (0)316 873 10 32339.
E-mail address: p.handel@vam-austria.com (P. Handel).

http://dx.doi.org/10.1016/j.jpowsour.2014.05.080
0378-7753/© 2014 Elsevier B.V. All rights reserved.

prolonged cycle and calendar life of the battery [6,7]. Another problem arises, if the electrolyte is in contact with a positive electrode material such as lithium cobalt dioxide $LiCoO_2$, which facilitates the formation of toxic, fluorinated compounds [8].

Additionally, state-of-the-art electrolyte systems may decompose thermally. This phenomenon can be severely increased by traces of protic impurities, most notably water, due to the hydrolysis sensitivity of the P–F bonds of $LiPF_6$. In fact, the products of the endothermic equilibrium of $LiPF_6$ (Equations (1)–(4))) are preferably formed at higher temperatures, leading to the formation of hydrofluoric acid (HF) and subsequently to further degradation of electrolyte components [9,10].

$$LiPF_6\ (s) \rightleftharpoons LiF\ (s) + PF_5\ (g) \quad (1)$$

$$PF_5\ (g) + H_2O\ (l) \rightarrow O{=}PF_3\ (g) + 2HF\ (l) \quad (2)$$

$$O{=}PF_3\ (g) + H_2O\ (l) \rightarrow O{=}PF_2(OH)\ (l) + HF\ (l) \quad (3)$$

$$O{=}PF_3\ (g) + RCO_3R\ (l) \rightarrow O{=}PF_2(OR)\ (l) + RF\ (g) + CO_2\ (g) \quad (4)$$

Moreover, HF may attack parts of the electrodes or the SEI (e.g. lithium carbonate Li_2CO_3), which consequently could lead to a shortened cycle life or even to a failure of the battery [11].

$$2HF\ (l) + Li_2CO_3\ (s) \rightarrow 2\ LiF\ (s) + H_2CO_3\ (l) \quad (5)$$

Until now, several working groups focused on the autocatalytic decomposition cycle of $O{=}PF_3$, which depends on the organic carbonates used as solvents [10,12–18]. Carbon dioxide (CO_2), ethylene ($H_2C{=}CH_2$), fluorophosphoric acid ($O{=}PF(OH)_2$), difluorophosphoric acid ($O{=}PF_2(OH)$), dialkyl fluorophosphates ($O{=}PF(OR)_2$), alkyl difluorophosphates ($O{=}PF_2(OR)$), alkyl fluorides (RF) and oligoethylene oxides were identified as main decomposition products.

Besides, major research activities were spent in the development of conductive salts with superior thermal stability or hydrolysis sensitivity compared to $LiPF_6$ [19–21]. But due to the best compromise regarding ionic conductivity, SEI-formation, toxicity and passivation of the aluminum current collector, $LiPF_6$ will remain predominant on the battery market so far. Hence profound understanding of the thermal decomposition mechanism is mandatory and specific attention needs to be paid to the thermal stability of the conductive salt and its solvents.

Herein, the properties of 1 M $LiPF_6$ in a binary mixture of organic carbonates were monitored at 60 °C and ambient temperature for 4 weeks. This temperature was chosen according to the calendar life test described in the performance test procedure from HELIOS [22], whereas other working groups used even higher temperatures [12,13,23]. DEC and EC were chosen as solvents, since previous studies have shown that this composition leads to faster degradation compared to e.g. dimethyl carbonate (DMC) [12]. According to literature, an increase in protic impurities leads to a faster decomposition of electrolytes. In commercial lithium-ion batteries, these protic traces may origin, for example, from electrolyte solvents, poor quality of $LiPF_6$ (adsorbed HF), aqueous processing of electrode slurries or from the hygroscopy of most common cathode materials and subsequent insufficient electrode drying.

To show the influence of protic contamination on the thermal degradation in a battery-like environment, a certain amount of deionized water as well as of undried lithium iron phosphate powder (LFP) with a well-known water content were separately added to the chosen electrolyte system and air tightly sealed under argon atmosphere. Hereby, the addition of deionized water should simulate the infiltration of moisture by passive components like the electrolyte or the separator, while the addition of the LFP powder should demonstrate the impact of poorly dried active material. Furthermore, undried LFP powder may offer a catalytic surface in the degradation process in contrast to solely added deionized water.

Beside the water content, the housing of the samples turned out to be crucial in terms of electrolyte degradation. In this context, the impact of glass versus polymer surface on electrolyte aging was examined. NMR-spectroscopy, GC–MS and Headspace-GC–MS were used to determine the decomposition products. The altering total acid and water content was measured by acid–base and coulometric titration, respectively.

2. Experimental

All chemicals used were of highest purity available. $LiPF_6$ (Stella Chemifa Corp., battery grade) was used as received. DEC (Aldrich, ≥99%) and EC (Acros Organics, ≥99%) were distilled for further purification and dried by molecular sieve. Karl Fisher titration showed that the distilled organic carbonates contained less than 20 μg g^{-1} water. LFP contained 1400 μg g^{-1} water and was supplied by Clariant Int. Ltd.

An electrolyte solution containing 1 M $LiPF_6$ in EC:DEC (1:2, v/v) was prepared in an argon-filled glove box and stirred for 15 h. An exact amount of electrolyte was transferred into a multi-layer aluminum foil bag (pouch bag, 7.5 × 10 cm) and carefully sealed under argon atmosphere.

To show the influence of glass surface on thermal degradation, additional samples were filled in glass vials (Supelco®) and sealed. Further samples were flame-sealed under reduced pressure in Duran® NMR-tubes.

The impact of 1000 μg g^{-1} of deionized water and the impact of 1000 μg g^{-1} water incorporated in undried LFP were investigated on the aging of another solution of 1 M $LiPF_6$ in EC:DEC (1:2, v/v). Addition of 75 μg deionized water and 0.053 g undried LFP powder (which refers to 75 μg of water) to a certain amount of electrolyte occurred immediately before the pouch bags (7.5 × 10 cm) were sealed under argon atmosphere, respectively.

Thermal aging of all samples occurred at 60 °C in a compartment dryer and at ambient temperature, respectively (within 2 days up to 4 weeks).

All GC–MS spectra were recorded on an Agilent Technologies 7890 GC coupled with a mass selective detector 5975. Helium was used as carrier gas (constant flow rate: 1 mL min^{-1}). A HP-5MS capillary column (30 m × 0.32 mm × 0.25 μm) was used for separation. The injection of the gaseous samples for headspace measurements was performed manually (Hamilton samplelock™ syringe, 2 mL gas volume per sample, split ratio of 1:500) into the split/splitless injector and the compounds were separated between 40 and 180 °C (rate 10 °C min^{-1}). Dichloromethane (CH_2Cl_2) was chosen for determination of decomposition products in the liquid phase. Samples prepared in CH_2Cl_2 were injected via autosampler (split ratio of 1:100) and measured with a heating rate of 7 °C min^{-1} from 38 to 45 °C, 10 °C min^{-1} between 45 and 70 °C, and 20 °C min^{-1} from 70 to 200 °C. The mass spectrometer operated in electron ionization (EI) mode with an electron energy of 70 eV. For data acquisition and processing MSD Chem Station E.02.01.117 (Agilent) and NIST spectra library was used.

Homo- and heteronuclear NMR-spectroscopy was performed on a Varian Mercury 300 MHz spectrometer. Samples aged in pouch bags were transferred in screw-mountable NMR-tubes. External lock signal was provided by a C_6D_6 filled glass capillary since residual H_2O in D_2O appears close to decomposition products or carbonates within the ^1H NMR spectrum. ^1H and ^{13}C NMR spectra were referenced to the solvent residual signal, ^{19}F NMR spectra to

trichlorofluoromethane CCl_3F and ^{31}P NMR resonances to phosphoric acid H_3PO_4. Spin lattice relaxation time (T_1) was determined via inversion recovery experiment. For the recording of quantitative ^{19}F NMR spectra the time between two scans (d1) was adjusted to be tenfold T_1. Benzotrifluoride (Alfa Aesar, 99%) was used as internal standard. Processing of the data occurred with the software TopSpin 3.2 (Bruker).

The determination of the water content in liquid samples took place on a Mitsubishi Moisture Meter Model CA-100 by coulometric Karl Fisher titration. The water content of solid samples was determined by coulometric titration using a Mitsubishi Water Vaporizer Model VA-100 coupled to the CA-100. The total acid concentration was determined by acid–base titration reaction using water-free sodium carbonate Na_2CO_3 and highly purified water (Milli-Q, Millipore).

In general, all of the measurements were performed under reproducibility conditions (two to three fold determinations) with validated methods considering requested measurement range, accuracy and precision.

3. Results and discussion

3.1. Aging of the electrolyte in glass vials

3.1.1. NMR-spectroscopy

Lucht and coworkers [12] as well as Campion and coworkers [13] described recently the thermal decomposition at 85 °C of $LiPF_6$, 1 M $LiPF_6$ in EC, 1 M $LiPF_6$ in EC:DMC, 1 M $LiPF_6$ in EC:DEC:DMC, 1 M $LiPF_6$ in DEC and 1 M $LiPF_6$ in EMC. However, we focused on 1 M $LiPF_6$ in EC:DEC (1:2, v/v) as a distinct lithium-ion battery electrolyte. If it is sealed in Duran® NMR tubes, the ^1H, ^{19}F, ^{31}P, ^{13}C NMR spectra are in good agreement with the published results even if a lower decomposition temperature of 60 °C is used. As shown in Table 1, most of the decomposition products already occur after 48 h at elevated temperature (Eqs. (1)–(4)). Difluoro substituted compounds appear after two days, monofluoro substituted decomposition products are observed after 4 weeks at 60 °C. Monofluoro substituted degradation products develop if either O=PF_2(OH) is reacting with water or if O=PF_2(OEt) is reacting with further organic carbonate. Since signals in ^{31}P NMR spectra are overlapping, no clear phosphorus signal is identified for O=$PF(OH)_2$ with a coupling constant of 926 Hz. The electrolyte samples aged at elevated temperature in sealed Duran® NMR tubes turn yellowish to brownish with increasing time. This change in color may result from the increasing amount of alkylated mono- and difluorinated decomposition products (π-bonding). Further, a white precipitate, which is identified as LiF, is formed on the bottom of the NMR tubes.

3.1.2. Headspace-GC–MS

Owing to the applied column, acid decomposition products such as fluorophosphoric acids cannot be identified via GC–MS.

Concerning the electrolyte decomposition in glassy headspace vials, phosphoryltrifluoride (m/z = 104, 85, 69) is present in the background of the electrolyte without any additives. After two days at 60 °C the gaseous phase of the thermally aged electrolyte contains Et_2O (m/z = 59, 45, 31), O=PF_2(OEt) (m/z = 115, 103, 85) and O=$PF(OEt)_2$ (m/z = 155, 127, 81), as shown in Table 2. As for samples aged in Duran® NMR tubes, the change of color is also apparent in glassy Headspace-GC–MS vials and white precipitate forms on the bottom.

3.2. Aging with and without added protic impurities in pouch bags

3.2.1. NMR-spectroscopy

In contrast, aging of the electrolyte in a pouch bag has not led to any detectable decomposition products, except for the difluorinated phosphoric acid (O=PF_2(OH)). No significant enhancement of its peak intensity is observed after 4 weeks at 60 °C compared to the freshly prepared electrolyte. The addition of undried LFP or the direct addition of 1000 μg g^{-1} deionized water only leads to the decomposition product O=PF_2(OH) (Fig. 1). A minor increase in the peak intensity of O=PF_2(OH) is only detected when deionized water is the protic impurity source. No change of color of the electrolyte samples is observed. To determine the increase in decomposition product O=PF_2(OH) quantitatively, inversion recovery experiments are recorded for the electrolyte samples. Benzotrifluoride (std) is used as internal standard and quantification of the total amount of O=PF_2(OH) occurs according to the following equation

$$m_{O=PF_2(OH)} = I_{OPF_2(OH)} \Big/ I_{std} * N_{std} / N_{O=PF_2(OH)} * M_{O=PF_2(OH)} / M_{std} * m_{std} * P_{std} / 100$$

where m is the mass, I the intensity of the integrals, N the number of NMR active nuclei in the structure, M the molecular weight and P the purity of the internal standard. Direct addition of 1000 μg g^{-1} deionized water leads to an approximate increase of 75% of O=PF_2(OH) peak intensity upon aging at 60 °C for 4 weeks compared to its initial concentration, although its concentration in the electrolyte samples is still nominal.

3.2.2. Headspace-GC–MS

After 4 weeks exposition at elevated temperature in a pouch bag, the electrolyte samples without added protic impurities only contain traces of Et_2O (m/z = 59, 45, 31) and traces of O=PF_2(OEt) (m/z = 115, 103, 85). As shown in Fig. 2, the direct addition of 1000 μg g^{-1} H_2O to the electrolyte samples leads to the formation

Table 1
Overview of decomposition products occurring in 1 M $LiPF_6$ in EC:DEC (1:2, v/v) upon aging at 60 °C in flame sealed, Duran® NMR tubes (^{19}F- and ^{31}P NMR spectra).

Exposure time	Nucleus	δ/ppm	m	J/Hz	Species
2 Days	$^{19}F/^{31}P$	−74.2/−144.4	d/sept	708/708	$LiPF_6$
	$^{19}F/^{31}P$	−85.0/−19.9	d/t	947/947	O=PF_2(OH)
	$^{19}F/^{31}P$	−86.0/−20.8	d/t	1005/1005	O=PF_2(OEt)
	$^{19}F/^{31}P$	−89.5/−34.8	d/q	1068/1068	O=PF_3
	^{19}F	−156.4	s		HF
28 Days[a]	$^{19}F/^{31}P$	−85.1/−10.4	d/d	961/961	O=$PF(OEt)_2$
	^{19}F	−87.15	d	926	O=$PF(OH)_2$
	^{19}F	−212.5	tq	47.9 (CH_2); 26.7 (CH_3)	EtF

[a] Additional decomposition products to those already occurring after 2 days at 60 °C.

Table 2
Summary of decomposition products of 1 M $LiPF_6$ in EC:DEC (1:2, v/v) detected upon aging at 60 °C either in different packaging materials or when 1000 μg g^{-1} protic impurities (deionized water or LFP) are added to the electrolyte in a pouch bag.

Species	Glassy/Duran® surface	Polymer surface	$+H_2O$	+LFP
$O{=}PF_2(OH)$	2 days (NMR)	2 days (NMR)	2 days (NMR)	2 days (NMR)
$O{=}PF_2(OEt)$	2 days (NMR, HS-GC–MS)	28 days (HS-GC–MS)	28 days (HS-GC–MS)	–
$O{=}PF_3$	2 days (NMR)	–	–	–
HF	2 days (NMR)	–	–	–
$O{=}PF(OEt)_2$	2 days (HS-GC–MS) 28 days (NMR)	–	–	–
$O{=}PF(OH)_2$	28 days (NMR)	–	–	–
EtF	28 days (NMR)	–	–	–
Et_2O	2 days (HS-GC–MS)	28 days (HS-GC–MS)	28 days (HS-GC–MS)	28 days (HS-GC–MS)
EtOH	–	–	28 days (HS-GC–MS)	28 days (HS-GC–MS)
Hydrocarbons	–	–	28 days (HS-GC–MS)	28 days (HS-GC–MS)
2-Fluoro-2-methylpropane	–	–	28 days (HS-GC–MS)	28 days (HS-GC–MS)

of ethanol EtOH (m/z = 45, 31, 15), Et_2O (m/z = 59, 45, 31) and a slight amount of $O{=}PF_2(OEt)$ (m/z = 115, 103, 85) in the gaseous phase. Moreover some hydrocarbons are identified like 2-methylprop-1-ene (m/z = 56, 41, 39), 2-fluoro-2-methylpropane (m/z = 61, 41), *(E)*-4-methylpent-2-ene (m/z = 84, 69, 41) and its tautomer 2-methylpent-2-ene (m/z = 84, 69, 41), 2.4.4-trimethylpent-1-ene (m/z = 112, 97, 57) and its tautomer 2.4.4-trimethylpent-2-ene (m/z = 112, 97, 55). Further investigation on the reaction mechanism is required. The addition of undried LFP leads to the formation of 2-methylprop-1-ene (m/z = 56, 41, 39), traces of 2-fluoro-2-methylpropane (m/z = 61, 41), traces of EtOH (m/z = 45, 31, 15) and Et_2O (m/z = 59, 45, 31) after the electrolyte samples are aged for 4 weeks at 60 °C. Table 2 illustrates the influence of different housing materials and addition of protic impurities on degradation at 60 °C. It's evident that most of the decomposition products are detected if aging occurred in glass vials.

Since electrolyte samples diluted in CH_2Cl_2 only contain a slight amount of $O{=}PF_2(OEt)$ (m/z = 115, 103, 85) after 4 weeks at 60 °C, they are not discussed within this paper. Further, as shown by NMR-studies, $O{=}PF_2(OH)$ is the main decomposition product after 4 weeks of aging at ambient and at elevated temperatures (Fig. 3). Since NMR-spectroscopy is less sensitive than GC–MS, decomposition products such as Et_2O or $O{=}PF_2(OEt)$ cannot be identified using this technique because they only occur in trace quantities, if pouch bags are used as sample housing.

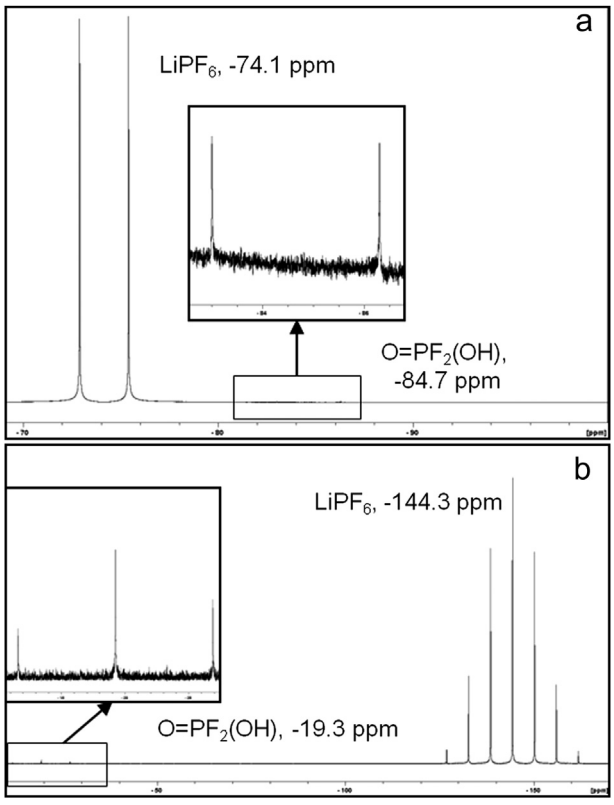

Fig. 1. NMR spectra of 1 M $LiPF_6$ in EC:DEC (1:2, v/v) aged at 60 °C for 4 weeks. (a) ^{19}F NMR and (b) ^{31}P NMR.

3.2.3. Titration methods

As shown by Heider et al. [11], the impact of higher temperature onto the electrolytes generally leads to a faster decrease in water content accompanied by a faster increase in total acid content. Exactly this behavior is followed by acid–base titration and coulometric Karl Fisher titration. During aging the total amount of free acid evolves steadily, depending on the initial concentration of protic impurities and temperature. Hence the higher the applied

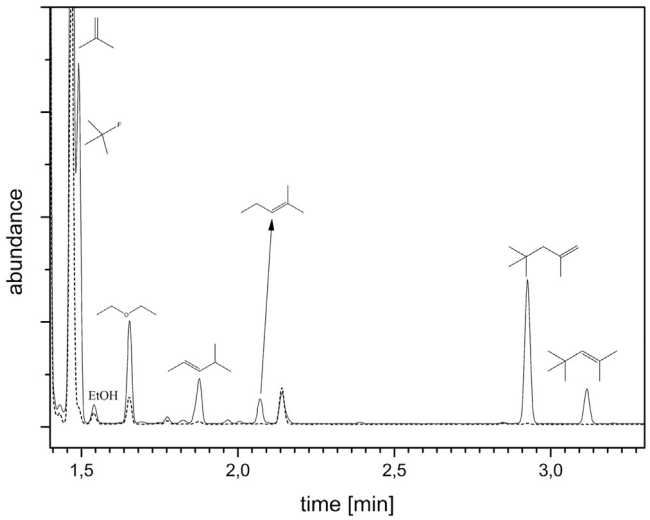

Fig. 2. Headspace chromatograms of 1 M $LiPF_6$ in EC:DEC (1:2, v/v) aged at 60 °C for four weeks containing either 1000 μg g^{-1} of deionized water (black, solid line) or 1000 μg g^{-1} water incorporated in LFP (black, dotted line).

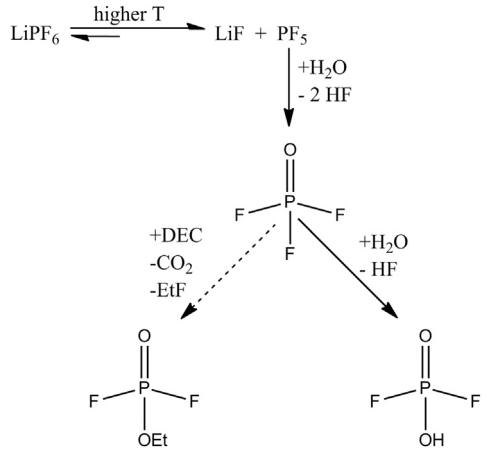

Fig. 3. Decomposition pathway of 1 M $LiPF_6$ in EC:DEC (1:2, v/v) in pouch bag at 60 °C. Degradation occurs at a very slow rate, leading mainly to difluorophosphoric acid.

temperature and the higher the concentration of protic impurities, the more conductive salt decomposition is caused as shown by Fig. 4.

No acceleration of the electrolyte degradation is visible either at ambient or elevated temperature when undried LFP is added. Thus, at ambient and elevated temperature the incorporated water in the LFP remains within the powder.

4. Conclusion

The thermal stability and the hydrolysis sensitivity of $LiPF_6$, one of the most common conductive salt used in electrolytes, remains one of the main problems for long-term performance of lithium-ion batteries so far. Herein, we investigated the behavior of an electrolyte without and with addition of deionized water or undried positive electrode material at ambient and elevated temperature.

The aging of electrolytes in air tightly sealed pouch bags mostly resemble the environment of a commercial lithium-ion battery and are closest to real application. Upon aging of 1 M $LiPF_6$ in EC:DEC (1:2, v/v) a significant increase in concentration of $O{=}PF_2(OH)$ was only followed either by NMR-spectroscopy or by acid–base titration if 1000 μg g^{-1} of deionized water was added to the electrolyte. Although some decomposition of the electrolyte with added deionized water occurred at ambient and elevated temperature, hardly any esterification reaction of $O{=}PF_3$ was observable after 4 weeks at 60 °C. Undried LFP powder had no influence on the enhancing total acid amount compared to the electrolyte without added LFP powder. Headspace-GC–MS showed that decomposition products mainly occurred in the gaseous phase when protic impurities were added.

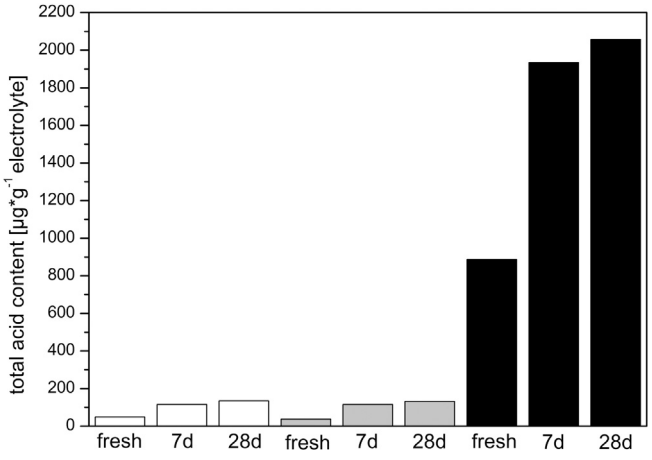

Fig. 4. Comparison of electrolyte degradation and evolvement of free acids at 60 °C for the pure electrolyte (white), 1000 μg g^{-1} water incorporated in LFP (gray) and 1000 μg g^{-1} of water (black) up to 28 days at 60 °C. The pure electrolyte and the electrolyte with added LFP powder follow the same trend.

Therefore, aging of 1 M $LiPF_6$ in EC:DEC occurs at a rather low speed as far as influencing variables such as catalytic surface, ambient air, protic impurities and too high temperature are excluded. Prospective studies regarding electrolyte decomposition should preferably avoid these influencing variables. Only if the electrolyte is in contact with glass surface during aging the results of NMR-spectroscopy and GC–MS distinguish tremendously from the electrolyte aged in sealed pouch bags. It's obvious that this environment accelerates the decomposition rate and after the storage in flame sealed Duran® NMR tubes or scrambled glassy Headspace-GC–MS vials for 4 weeks at 60 °C even monofluorinated products were observed. We believe that HF reacts with silicon dioxide SiO_2 to form silicon tetrafluoride SiF_4 and water. The generated water leads to further electrolyte decomposition.

Acknowledgment

VAM Entwicklungs GmbH and VOLKSWAGEN VARTA Microbattery Forschungsgesellschaft are gratefully acknowledged for funding.

References

[1] T. Yamahira, H. Kato, M. Anzai, Nonaqueous Electrolyte Secondary Battery, US5053297 A, Japan, 1990.
[2] D. Aurbach, B. Markovsky, A. Rodkin, M. Cojocaru, E. Levi, H.-J. Kim, Electrochim. Acta 00 (2002) 1–13.
[3] K. Xu, Chem. Rev. 104 (2004) 10.
[4] D. Aurbach, B. Markovsky, G. Salitra, E. Markevich, Y. Tolyossef, M. Koltypin, L. Nazar, B. Ellis, D. Kovacheva, J. Power Sources 165 (2007) 491–499.
[5] G. Gachot, S. Grugeon, G.G. Eshetu, D. Mathiron, P. Ribieère, M. Armand, S. Laruelle, Electrochim. Acta 83 (2012) 402–409.
[6] E. Peled, J. Electrochem. Soc. 126 (1979) 2047–2051.
[7] W. Li, B.L. Lucht, J. Electrochem. Soc. 153 (2006) A1617–A1625.
[8] A. Hammami, N. Raymond, M. Armand, Nature 424 (2003) 635–636.
[9] S.F. Lux, I.T. Lucas, E. Pollak, S. Passerini, M. Winter, R. Kostecki, Electrochem. Commun. 14 (2012) 47–50.
[10] J.S. Gnanaraj, E. Zinigrad, L. Asraf, H.E. Gottlieb, M. Sprecher, M. Schmidt, W. Geissler, D. Aurbach, J. Electrochem. Soc. 150 (11) (2003) A1533–A1537.
[11] U. Heider, R. Oesten, M. Jungnitz, J. Power Sources 81–82 (1999) 119–122.
[12] C.L. Campion, W. Li, B.L. Lucht, J. Electrochem. Soc. 152 (12) (2005) A2327–A2334.
[13] B. Ravdel, K.M. Abraham, R. Gitzendanner, J. DiCarlo, B. Lucht, C. Campion, J. Power Sources 119–121 (2003) 805–810.
[14] A. Xiao, W. Li, B.L. Lucht, J. Power Sources 162 (2006) 1282–1288.
[15] K. Tasaki, K. Kanda, S. Nakamura, M. Ue, J. Electrochem. Soc. 150 (12) (2003) A1628–A1636.
[16] L. Terborg, S. Weber, F. Blaske, S. Passerini, M. Winter, U. Karst, S. Nowak, J. Power Sources 242 (2013) 832–837.
[17] S. Wilken, M. Treskow, J. Scheers, P. Johansson, P. Jacobsson, RSC Adv. 3 (2013) 16359–16364.
[18] B. Vortmann, S. Nowak, C. Engelhardt, Anal. Chem. 85 (2013) 3433–3438.
[19] D. Aurbach, Y. Talyosef, B. Markovsky, E. Markevich, E. Zinigrad, L. Asraf, J.S. Ganaraj, H.-J. Kim, Electrochim. Acta 50 (2004) 247–254.
[20] L. Yang, C. Smith, C. Patrissi, C.R. Schumacher, B.L. Lucht, J. Power Sources 185 (2008) 1359–1366.
[21] G.G. Eshetu, S. Grugeon, G. Gachot, D. Mathiron, M. Armand, S. Laruelle, Electrochim. Acta 102 (2013) 133–141.
[22] M. Mettlach, HELIOS – High Energy Lithium-ion Storage Solutions – Cell Test Specification, 2012, p. 11.
[23] H. Yang, G.V. Zhuang, P.N. Ross Jr., J. Power Sources 161 (2006) 573–579.